AD-A159 912 SURFACE AND INTERFACIAL PROPERTIES OF INP(U) CALIFORNIA 1/1
UNIV SAN DIEGO LA JOLLA DEPT OF ELECTRICAL ENGINEERING
AND COMPUTER SCIENCES L G MEINERS ET AL. 31 APR 85
UNCLASSIFIED N00014-82-K-2032 F/G 20/12 NL

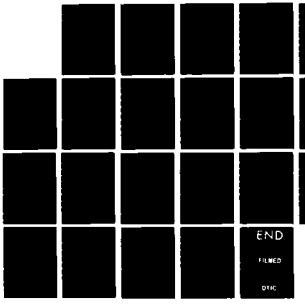

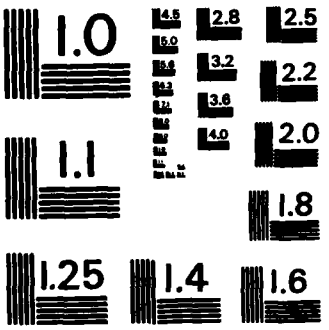

MICROCOPY RESOLUTION TEST CHART
NATIONAL BUREAU OF STANDARDS-1963-A

Final Report

Contract No. N000-82-K-2032

Naval Research Laboratory (Mr. Howard Lessoff, Electronics Materials Technology Branch, Code 6820).
Washington D. C. 20375

Surface and Interfacial Properties of InP

Co-principal Investigators: L. G. Meiners and H. H. Wieder

Department of Electrical Engineering and Computer Sciences, C-014
University of California, San Diego
La Jolla, CA 92093

Abstract

The enclosed reports represent work performed at UCSD on Contract N00014-82-K-2032 entitled "Surface and Interfacial Properties of InP" and provides a full account of the results obtained during the contract period: May 1, 1984 through April 31, 1985. The paper "Space charge-limited currents and trapping in semi-insulating InP" has now been published in Electron. Device Letters, volume EDL-6, page 356 (1985). The manuscript "Effect of bulk traps on the InP accumulation type MISFET" will be presented as an invited talk at the fall meeting of the Electrochemical Society in Las Vegas, October 14-17 and will be published in the Journal of the Electrochemical Society.

The Effect of Bulk Traps on the InP Accumulation Type MISFET

L. G. Meiners

Department of Electrical Engineering and Computer Sciences

C-014

University of California, San Diego

La Jolla, CA 92093

Abstract

Calculations of the effect of bulk traps on the time dependence of the channel current in InP accumulation-type MISFET's are reported. It is shown that a uniform density of deep acceptors in the bulk material given rise to a decay in the channel current which decays approximately linearly as a function of the logarithm of time. If capture of the electrons is assumed to occur by a nonradiative multiphonon emission process, then the temperature dependence that is obtained agrees with experimental results.

Cont'd on Pg. 356

Introduction

Indium phosphide (InP) is an attractive material for the fabrication of metal-insulator-semiconductor (MIS) field-effect transistor (FET) because of its large saturated drift velocity for electrons and the favorable conditions present at its oxide-semiconductor interface. While efforts to construct MISFETs on gallium arsenide were unsuccessful due to the large interface state density on this material[1,2], progress has been much more rapid in the case of InP. Interface state densities between deposited layers of silicon dioxide (SiO_2) and InP have been calculated to be as low as 2×10^{11} $cm^{-2}eV^{-1}$ based on capacitance-voltage measurements on MIS diodes[3,4,5]. A type of MISFET which has been labeled the accumulation-type device has been realized on InP[6]. Construction of this device begins with the formation of two heavily doped (n^+) ohmic contacts for the source and drain regions on a wafer of semi-insulating (SI) InP. The wafer is then coated with a thin insulating layer, overlapping gate electrodes are evaporated on top of the insulator and windows are etched through the insulator for connection to the source-drain electrodes. A cross-sectional view of the device is shown in Fig. 1. This device was originally proposed and fabricated because the reduced capacitance between the conducting channel and the substrate was expected to lead to a better high frequency response than similar devices constructed on p-type substrate material. Indeed, this was found to be the case.

A remaining problem to be solved before the device is perfected is a long-term drift in the drain current that is observed when a constant voltage is applied between the gate and source electrodes[7,8]. Several models have been proposed which attempt to explain the origin of the drift by tunneling currents between states in the insulator and the conduction band of the semiconductor[9,10,11]. I feel that these models have serious shortcomings and

that although they give substantially correct mathematical expressions for the current drift they have errors in their formulation. This is further discussed in the paper.

A first order model for the I-V behavior of the accumulation-type transistor based on the gradual channel approximation has been formulated by Wieder[12]. His model assumed that the substrate (the SI InP) could be treated as an ideal insulator.

In this paper I present calculations for the time-dependent behavior of the accumulation-type transistor which take into account the fact that the conducting channel of the device is on the surface of a semiconductor which contains both shallow donors (due to native defects) and deep acceptors (introduced by iron doping). The time dependence of the device is calculated by assuming that the capture and emission of electrons by the bulk impurity states is governed by a Shockley-Read type of recombination process. Poisson's equation has been solved numerically to obtain the time development.

Background

The key features which must be explained by any proposed model for drift of the channel current in the accumulation-type transistor are illustrated in data published by Lile, et al.[7] which are reproduced in Fig. 2. The channel current decays linearly as a function of the logarithm of time and the capture process "freezes out" at low temperature. Clearly a tunneling process as decribed by Heiman and Warfield[13] cannot explain such data since there would be no temperature dependence if electrons were to tunnel from conduction band states to oxide trap levels at the same energy.

One of the proposed models for explaining the current drift in the accumulation-type transistor as presented by Goodnick, et al.[9] is attractive

because it is based on physical evidence that the interface of InP coated with deposited SiO_2 consists of multiple layers as shown in Fig. 3a. They proposed that the layer immediately adjacent to the InP consists of a relatively large bandgap material ($InPO_4$) which is covered with a lower bandgap material (In_2O_3) which in turn is covered with SiO_2. When a positive voltage is applied to the gate of the device to form the conducting channel in the SI InP, they proposed that a thermally-assisted tunneling current flows from the semiconductor to states in the In_2O_3. Their solution for the channel current (I_d) as a function of time gives a linear dependence of I_d on log t. The temperature dependence is obtained in their model from the experimentally measured conduction band offset between the InP and the In_2O_3. Wager et al.[14] concluded from photoemission (XPS, UPS) and electron-loss spectroscopy (ELS) measurements of deposited SiO_2 layers on InP that the conduction band minimum in the native oxide In_2O_3 is 0.1 to 0.2 eV higher than in InP. In the Goodnick, et al. thermally-assisted tunneling model, the electrons can tunnel from the InP to the In_2O_3 only if their kinetic energy is greater than the energy barrier step from the InP to the In_2O_3. As the temperature is reduced fewer electrons are able to surmount this barrier and the drift effect decreases. However, this model fails to take into account the fact that with a positive voltage on the gate electrode there will be a voltage drop across the $InPO_4$ layer and a lowering of the conduction band of the In_2O_3 as shown in Fig. 3b. Once the conduction band of the In_2O_3 is below the conduction band of the InP all the temperature dependence of the I_d vs. t curves would disappear. For a 40 Å layer of $InPO_4$ as assumed in their calculation this requires a gate voltage of $V_g \simeq . 2(d_{SiO_2} + d_{InPO_4})/d_{InPO_4} = 5.2$ volts. In this very rough estimate, d_i represents the thickness of the $InPO_4$ and SiO_2 layers, the dielectric constants of the two layers have been assumed equal, and the amount of conduction

band offset has been assumed to be, as an upper limit, 0.2 v. The temperature dependence of the drift current should then disappear for gate voltages larger than about 5 v. This is contrary to the experimental evidence. At low temperature the current drift disappears for all values of gate voltage. One could attempt to salvage this model by reducing the thickness of the $InPO_4$ layer so as to minimize the voltage drop across it. However, this would at the same time eliminate the tunneling barrier and eliminate the log t dependence of I_d. Alternatively, one could assume a lower resistivity of the $InPO_4$ layer so that the voltage drop across it would be less, but this would again eliminate the tunneling behavior needed to get the proper time dependence.

Okamura and Kobayashi[10] have proposed that the current drift in the accumulation type device can be explained by thermally-assisted tunneling from the conduction band of the InP into a pair of electron trap levels in the insulator. The energy band diagram relevant to their scheme is shown in Fig. 4. They base their calculation on a model originally proposed by Koelmans and DeGraaff[15]. This model begins by assuming that the charge flow into the oxide trap can be represented by a Shockley-Read[16] type of recombination rate equation, viz:

$$\frac{dn_{tr}}{dt} = S(x)\,\bar{v}\,[n_s\,(N_{tr} - n_{tr}) - n_1\,n_{tr}] \qquad (1)$$

where n_s is the electron concentration at the interface, n_{tr} is the density of filled traps, $\bar{v}$ is the average thermal velocity of the electrons and N_{tr} is the total trap density. The quantity n_1, is given by the equation

$$n_1 = N_c\,e^{-(E_{cs} - E(x))/kT} \qquad (2)$$

where N_c is the effective density of states for the conduction band, k is Boltzmann's constant, T is the absolute temperature, and E_{cs} and E(x) are energies defined in Fig. 4. This particular value of n_1 must be used if the principle of detailed balance is to be maintained. That is, at thermal equilibrium

$$\frac{dn_{tr}}{dt} = 0 \tag{3}$$

which then implies that

$$n_1 = \frac{n_s (N_{tr} - n_{tr})}{n_{tr}} \tag{4}$$

Since

$$n_s = N_c e^{(E_{cs})/kT} \tag{5}$$

and

$$\frac{N_{tr} - n_{tr}}{n_{tr}} = e^{E(x)/kT} \tag{6}$$

analagous to the equation for the ratio of ionized donors to unionized donors for an impurity state in a semiconductor[17], one is forced to choose Eq. (2) to represent n_1 in order to satisfy the detailed balance requirement. The tunneling current is modeled by assuming that the charge flow into the oxide traps can be accounted for by a capture cross section which is an exponential function of distance into the oxide, i.e.

$$S(x) = S_o e^{-ax} \tag{7}$$

where 1/a represents a tunneling length. In this picture the probability that an electron at the surface will tunnel into an oxide trap is represented by the product of the electron density at the surface, the thermal velocity, the number of empty traps at distance x into the oxide, and the distance-dependent

capture cross section. Koelmans and DeGraaff solve this equation to obtain an equation for the total trapped charge density, ($N_e(t)$), as a function of time (t) which is of the form

$$N_e(t) = \frac{N_{tr}}{a} \ln (t/t_o) \tag{8}$$

where t_o is a constant. The original model as formulated by Koelmans and DeGraaff gives no temperature dependence to the tunneling current.

The modification to this model as proposed by Okamura and Kobayashi includes a trap level in the oxide which is placed above the conduction band of the InP by an energy ($E_s^{(2)} - E_{cs}$). They reasoned that only the more energetic conduction band electrons would be able to be captured by these traps and that the capture rate would be reduced by a factor $e^{-(F_s(2) - E_{cs})/kT}$. If the Shockley-Read equation is solved using their capture cross section, then the charge trapped by this level is given by

$$N_e = \frac{N_{tr}^{(2)}}{a^{(2)}} e^{-E_s^{(2)}/kT} \ln(t/t_o). \tag{9}$$

However, their derivation neglects the constraint that detailed balance imposes on the formulation of the Shockley-Read rate equation. If the rate equation is required to satisfy the requirement that

$$\frac{dn_{tr}^{(2)}}{dt} = 0 \tag{10}$$

at thermal equilibrium then the term $n_1^{(2)}$ in the emission rate expression must be changed to

$$n_1^{(2)} = N_c\, e^{-(E_s^{(2)} - E_{cs})/kT}\, e^{-(E_{cs} - E_{(x)})/kT}$$

$$= N_c\, e^{-(E_s^{(2)} - E_{(x)})/kT} . \qquad (11)$$

This is mathematically equivalent to assuming a smaller capture cross section for the trap. When the rate equation is solved with this reformulation there is again no temperature dependence of the trapped charge density. This is consistent with the paper of Koelmans and DeGraaff[15] since they formulated their model assuming that the trap level was placed at an arbitrary position in the forbidden energy gap and obtain the generalized result, that the trapping of electrons in the oxide is not temperature dependent. The question of whether or not one is justified in neglecting the detailed balance requirement will be addressed later in the paper.

Yamaguchi, et al.[11] have calculated the tunneling current into the oxide using a model similar to the original Koelmans and DeGraff model. Although they employ a different calculation scheme, their model like the Koelmans and DeGraff model contains no element for predicting the experimentally observed temperature dependence of the drift current.

Given the problems that have been encountered in devising a model which simultaneously gives the correct time and temperature of the drift current in the accumulation-type transistor when the charge trapping mechanism is placed in the insulator, it is interesting to consider an alternate approach which places the charge trapping mechanism in the semiconductor. How do we know that the charge is being trapped in the insulator? The answer is that we don't. The extant published data do not rule out the possibility that the charge trapping may occur in the semiconductor. The next point to consider is that the accumulation-type device has as its basis an electric field induced

layer of electrons on the surface of an InP SI crystal. The InP substrate material has a background concentration of unintentionally introduced hydrogenic donors which are located 7 to 10 meV below the conduction band minimum (E_c) [18] and have a density which is of the order of 2×10^{15} cm^{-3}. In the near surface region, phosphorus vacancies may also exist. These are thought to give rise to an energy level 0.1 eV below E_c [19]. In these calculations E_d was placed 0.1 eV below E_c although the results were not particularly sensitive to the value used for this parameter. The origin of these native donors is at the present time unknown. During the growth of the crystal, iron is added to the melt to produce deep compensating acceptors which are located approximately 0.68 eV above the valence band maximum (E_v). As long as the deep acceptor density is greater than the background concentration of native donors, the material will be semi-insulating. As the present time, commercially available SI InP is not sold with clearly specified upper limits to the amount of iron which may be present. Consider now Fig. 5 which illustrates the energy band diagram of an SI InP substrate biased such that the surface is accumulated. If the material is fully compensated and the bands are flat, then at thermal equilibrium nearly all the donors ($N_{di} \approx N_d$) will be ionized but only a fraction ($N_{ai} \approx N_d$) of the acceptors will be ionized. The ionized donor density will be given by

$$N_{di} = \frac{N_d}{1 + g_d \, e^{(E_F - E_d)/kT}} . \qquad (12)$$

the ionized acceptor density will be given by

$$N_{ai} = \frac{N_a}{1 + 1/g_a \, e^{(E_a - E_F)/kT}} \qquad (13)$$

the electron density will be given by

$$n = N_c \, e^{-(E_c - E_F)/kT} \tag{14}$$

and the hole density will be given by

$$P = N_v \, e^{-(E_F - E_v)/kT} . \tag{15}$$

In these equations $g_{d,a}$ represents the degeneracy of states for donors and acceptors respectively, E_F represents the position of the Fermi level with respect to E_v in the neutral bulk material, $E_{d,a}$ represents the energy of the donor and acceptor levels respectively as measured with respect to E_v, N_c represents the effective density of states at $E = E_c$ for electrons and N_v represents the effective density of states at $E = E_v$ for the holes. The position of the Fermi level can be readily calculated by numerically solving the equation

$$\rho = -n + p + N_{di} - N_{ai} = 0. \tag{16}$$

for E_F and using equations 12, 13, 14 and 15 to solve for the desired quantities. If N_a is greater than several times N_d and E_d is greater than E_v by several kT, then to a good approximation

$$E_F = E_A - \frac{kT}{q} \ln \frac{2(N_a - N_d)}{N_d} . \tag{17}$$

When a positive voltage is applied to the gate electrode of an MOS device on SI InP, the energy bands will bend downward as shown in Fig. 5. Notice

that acceptor states near the surface that were formerly above the Fermi level are now pushed downward by electric field. As this happens electrons will fill the empty acceptor states causing them to be completely ionized in the near surface region. If the gate voltage is held constant, then the electric field which now terminates on the additionally ionized acceptors will clearly cause a reduction in the mobile channel charge. This process would lead to a reduction of the channel current of an FET over time and could easily be mistaken for interfacial charging. The remainder of this paper presents numerical calculations of the time dependence of this drift effect under various conditions.

Theory

The first step in the formulation of this model is the assumption that n^+ ohmic contacts are present on the surface of the semiconductor and that the gate electrode partially overlaps these contacts. This is the typical state of affairs for the accumulation-type MISFET. This assumption is essential from a physical standpoint because the n^+ contact provides for easy transfer of electrons in and out of conduction band states and is essential for the formulation of the model because it permits the electron density to be described by an equilibrium Fermi level. The generation recombination processes were assumed to be characterized by the Shockley-Read rate equations[16].

$$\frac{dN_{di}(x)}{dt} = C_d\left[-N_{di}(x)n_b\, e^{q\psi/kT} + \frac{N_c}{2} e^{(E_d - E_c)/kT}(N_d - N_{di}(x))\right] \qquad (18)$$

and

$$\frac{dN_{ai}(x)}{dt} = C_a\left[(N_a - N_{ai}(x))n_b\, e^{q\psi/kT} - \frac{N_c}{2} e^{(E_a - E_c)/kT} N_{ai}(x)\right] \qquad (19)$$

where C_d and C_a represent capture coefficients given by $\bar{v}\sigma_d$ and $\bar{v}\sigma_a$ respectively, n_b represents the electron density in the bulk material, ψ is the static potential and σ_d and σ_a represents the capture cross sections for the donors and acceptors respectively. Both the donor and acceptor impurity states were assumed to be doubly degenerate. The boundary conditions were as follows: it is assumed that the fixed interfacial charge is equal to zero and that the work function difference between the metal and the semiconductor is equal to zero. A gate voltage $V_g = 0$ is applied for $t<0$ and a fixed positive gate voltage is applied for $t > 0$. With these boundary conditions

$$N_{di}(x)\Big|_{t=0} \tilde{=} N_d \quad \text{and} \quad N_{ai}(x)\Big|_{t=0} \tilde{=} N_d. \tag{20}$$

The value of the surface potential at $t = 0^+$ was obtained by solving the equation

$$V_g = \psi_s + \frac{Q_s + Q_{ss}}{C_{ox}} = \psi_s + \frac{\epsilon_s E_s}{C_{ox}} + \frac{Q_{ss}}{C_{ox}} \tag{21}$$

where Q_s and E_s are respectively the total charge on the semiconductor and the surface electric field, Q_{ss} is the charge in surface states and C_{ox} is the oxide capacitance per unit area. For the calculated results presented herein it has been assumed that $Q_{ss} = 0$. The effect of a non-zero threshold voltage (V_{th}) can be obtained in this model by assuming a non-zero fixed value of Q_{ss}. The boundary condition V_g = constant would then be replaced with the boundary condition $V_g - \frac{Q_{ss}}{C_{ox}}$ = constant. At $t = 0^+$ the ionized donor and acceptor densities were assumed not to have changed from their values for $t \leq 0$. The equation for the surface electric field as shown below[20]

$$E = -\frac{d\psi}{dx} = \left(\frac{2kT}{\epsilon_s}\right)^{1/2} [n_b(e^{q\psi/kT} - 1)$$

$$+ N_d \ln \left[\frac{2 + e^{(-q\psi + E_c - E_d - E_F)/kT}}{2 + e^{(E_c - E_d - E_f)/kT}} \right]$$

$$+ N_a \ln \left[\frac{2 + e^{(E_f - E_a - E_v + q\psi)/kT}}{2 + e^{(E_f - E_a - E_v)/kT}} \right] + p_b (e^{-q\psi/kT} - 1) \Big]^{1/2} \qquad (22)$$

reduces to

$$E = -\frac{d\psi}{dx} \approx \left(\frac{2kT\, n_b}{\varepsilon_s} \right)^{1/2} e^{q\psi/2kT} \qquad (23)$$

for $q\psi >> kT$; p_b, $n_b << N_a$, N_d, and $N_{di} \approx N_{ai}$.

The charge density distribution at $t = 0^+$ can be obtained explicitly by simultaneously solving Eqs. 21 and 23. Similarly the charge density distribution at $t = \infty$ can be obtained by simultaneously solving Eqs. 21 and 22. A graphical solution of these equations is indicated in Figs. 6 and 7. The E_s vs ψ_s curves at $t = 0^+$ and $t = \infty$ were calculated for specific donor and acceptor impurity densities. The intersection of these curves with a particular curve of constant V_g as formulated by Eq. 21 represents a particular solution. The area between the E_s vs ψ_s curves at $t = 0^+$ and $t = \infty$ represents the field of possible solutions for the time dependent problem. The decrease in the conducting channel carrier density can be obtained by noting the solution for ψ_s as indicated in Figs. 6 and 7. At $t = 0^+$ the total charge due to conduction band electrons is given to a good approximation by

$$Q_n \approx \varepsilon_s E_s \approx (2kT\varepsilon_s n_b)^{1/2} e^{q\psi_s/2kT}. \qquad (24)$$

At $t = \infty$ the mobile electron charge can be obtained by numerically integrating the equation

$$Q_n = q \int_0^\infty n(x)dx \qquad (25)$$

or its equivalent

$$Q_n = q\int_{\psi_s}^{0} \frac{n_b\, e^{q\psi/kT} d\psi}{(d\psi/dx)} \qquad (26)$$

where $d\psi/dx$ is given by Eq. 22 and ψ_s is obtained from from Figs. 6 or 7. Although Fig. 6 seemingly indicates that the solutions differ very little for large V_g, this is not quite the case. The solutions for ψ_s do differ by a small amount but since the mobile electron density depends exponentially on ψ_s, the difference in electron density can be large. The reduction in channel current for a range of acceptor concentrations is indicated in Fig. 8. It is instructive to consider calculated plots of the surface potential and electric field in Fig. 9 as a function of distance into the crystal. An unobvious point is that the electric field penetrates an extremely large distance ($w \approx 2$mm) into the material when the gate voltage is initially applied. This is due to the fact that initially only a small fraction of the acceptors are ionized and there are few charged centers for the electric field lines to terminate on. If a small geometry FET were being considered, the entire surrounding area of the FET would be affected by the field. Only after the deep acceptor levels near the surface have filled with electrons does the accumulation layer width shrink to device dimensions. The calculations presented here being one-dimensional in nature do not take into account such two dimensional geometry effects since the InP crystal has been assumed to be semi-infinite.

Solution of the time dependence of this problem begins by evaluating Eq. 22 at $\psi = \psi_s$, inserting this into Eq. 21 and solving the result iteratively using Newton's method to obtain ψ_s. The variation of ψ with position at $t = 0^+$ was obtained by integrating Eq. 23

$$\int_0^x dx = -\left(\frac{\varepsilon_s}{2kTn_b}\right)^{1/2} \int_{\psi_s}^{\psi(x)} e^{-q\psi kT} d\psi, \tag{27}$$

which yields

$$x = \left(\frac{2\varepsilon_s kT}{n_b q^2}\right)^{1/2} \left(e^{-q\psi(x)/2kT} - e^{-q\psi_s/2kT}\right) \tag{28}$$

which can be solved for $\psi(x)$ to give

$$\psi(x) = -\frac{2kT}{q} \ln\left[e^{-q\psi_s/2kT} + \left(\frac{n_b q^2}{2\varepsilon_s kT}\right) x\right]. \tag{29}$$

The carrier density at $t = 0^+$ is then obtained by inserting Eq. 29 into

$$n(x) = n_b e^{q\psi(x)/kT}. \tag{30}$$

The above equations were used to solve for the values of $\psi(x)$ and $n(x)$ on an array of points x_i with a variable spacing selected with the algorithm $x_0 = 0$, $x_1 = 10^{-10}$ m, $\Delta x_1 = 10^{-10}$ m, $x_{i+1} = x_i + \Delta x$; $\Delta x_{i+1} = \Delta x$; if $n(x_{i+1}) > 1.1n(x_i)$ and $\Delta x_{i+1} = 1.1\Delta x$; if $n(x_{i+1}) < 1.1\, n(x)$. The variable spacing is required in order to have closely spaced points near the surface where the carrier density drops rapidly and widely spaced points in the interior where the carrier density drops slowly.

Given initial values for $n(x)$, $N_{di}(x)$ and $N_{ai}(x)$, the time development of the trapped charge was approximated by using Eqs. 18 and 19 to obtain

$$N_{di}(x,t + \delta t) = N_{di}(x,t) + \frac{dN_{di}(x,t)}{dt} \delta t \tag{31}$$

and

$$N_{ai}(x,t + \delta t) = N_{ai}(x,t) + \frac{dN_{ai}(x,t)}{dt} \delta t. \tag{32}$$

With these new values of ionized impurity density Poisson's equation

$$\frac{d^2\psi}{dx^2} = -\rho/\varepsilon_s \tag{33}$$

can be solved numerically using a fourth-order Runge-Kutta method[21] given that the charge density is

$$\rho = q(-n + N_{di}(x,t + \delta t) - N_{ai}(x,t + \delta t)) \tag{34}$$

where

$$n = n_B\, e^{q\psi(x)/kT}. \tag{35}$$

The second-order differential equation can be reduced to the pair of coupled first-order equations given by

$$\frac{dE}{dx} = \rho/\varepsilon_s \tag{36}$$

and

$$\frac{d\psi}{dx} = -E. \tag{37}$$

In the solution of Eq. 32 for a new value of time, say $t = t + \delta t$, the first trial value of $\psi_s(t + \delta t)$ was set to $\psi_s(t)$. This value of ψ_s was used in Eq. 20 to solve for the trial value of $E_s(t + \delta t)$. These starting values of ψ_s and E_s were used in the Runge-Kutta procedure to solve for $\psi(x,t + \delta t)$ and $E(x,t + \delta t)$ from the surface inwards. If $\psi(x,t + \delta t)$ and $E(x,t + \delta t)$ reached zero simultaneously then ψ_s and E_s represent a solution. If $\psi(x,t + \delta t)$ reached zero before $E(x,t + \delta t)$, then ψ_s was too small and if $E(x,t + \delta t)$ reached zero before $\psi(x,t + \delta t)$ then ψ_s was too large. A new value of ψ_s was chosen that was known to lie between values of ψ_s that had been calculated to

be either too large or too small and the process was repeated until a solution was obtained.

Calculated results for the charge in conduction band states (N_s) as a function of time are shown in Fig. 10. The charge is nearly constant for very short times and then exhibits a decay which is nearly linear in log t. The time dependence of the calculated results is very similar to the data presented by Yamaguchi, et al[8] and by Lile, et al.[7] However, the temperature dependence is not as strong as observed in the measurements by Taylor, et al. The temperature dependence in the model just described is due to the reduction in the Debye length

$$L_D = \left[\frac{2kT\epsilon_s}{q^2 n_B} \right]^{1/2} \tag{38}$$

as the temperature is lowered. At low temperature the electrons crowd closer together at the surface and the electron density in the far surface region is reduced. This has the effect of reducing the magnitude of the terms due to electron capture in Eqs. 17 and 18. In order for a model based on trapping by bulk impurities to give the temperature dependence observed experimentally, it is necessary to introduce an energy barrier for electron capture. Clearly a model based on Fig. 5 cannot give the required temperature dependence. In this simplest formulation, the capture rate of electrons is given, for example, by

$$R_e = \bar{v}\sigma n N_{an} \tag{39}$$

which is mathematically equivalent to a statement that all that is required for an electron and a neutral acceptor to recombine is that they be in sufficiently close proximity to each other.

A model for nonradiative transitions in a crystal which can perhaps explain the observed behavior on SI InP was first proposed by Huang and Rhys[22] and expanded on by Kubo and Toyozawa[23] and by Rickayzen[24]. In this model it is assumed that the capture of an electron by a deep level impurity is accompanied by a local relaxation of the crystal lattice. In Fig. 11 the upper curve represents the total potential energy of the lattice plus free electron as a function of a generalized lattice coordinate Q. The curve represents schematically a hyper surface in 4-space. The lower curve represents the total potential energy of the lattice plus that of a trapped electron. The minima of the two curves are displaced due to the lattice relaxation which occurs when the electron is trapped. There are two processes by which an electron can transfer from the free to the trapped state. Classically it can undergo a transition if the lattice vibrations are large enough to cause the energy to cross point C on the upper curve. Since the system could be in either state and have the same value of energy and lattice coordinate there is finite probability that the electron will transfer from the free to the bound state. The activation energy for this process will be E_0. At low temperature when the transition probability via this path becomes small, the relative probability of direct tunneling from state Q" to A' and the subsequent emission of one or more phonons becomes larger. At T = 0 the optical transition energy would be E_0. The thermal activation energy for transition from the bound to free state is indicated by E_I. The applicability of this model for interpreting measurements on GaAs and GaSb has been discussed by Henry and Lang[25].

Seemingly an immediate consequence of proposing this model for the electron trap is that one is forced to abandon the concept that the principle of detailed balance will determine the relationship between the capture and

emission rates at steady state with no electric field applied. I hesitate to use the phrase thermal equilibrium to describe this condition because it seems as if this type of trap would not be in thermal equilibrium with the conduction band electrons. The relative magnitudes of the capture and emission coefficients would determine the density of occupied traps at steady state and the ratio of filled traps to the total number of traps can be used to define a quasi-Fermi level for the electrons in the traps. That this result would be the case can be argued by imagining that the energy E_o of the trap is increased as E_I is held constant. The capture rate would then decrease while the emission rate remained constant and the density of occupied traps would decrease. Since the Fermi energy for the electrons in conduction band states would be independent of the details of the trap configuration, seemingly the only way out is to describe the trap by a different quasi-Fermi level even in the steady state condition. The rate equation describing the dynamic behavior of this trap then becomes

$$\frac{dN_{ai}(x)}{dt} = C_a e^{-Eo/kT}(N_a - N_{ai}(x))n_b e^{q\psi/kT} - e_a N_c e^{-E_I/kT} N_{ai}(x) \quad (40)$$

where the functional form of the emission rate as proposed by Kubo[26] has been employed.

The calculation of the time dependence of the channel current for the accumulation MISFET was repeated using Eq. 35 for the dynamics of the electron capture by the deep acceptors and Eq. 17 for the capture dynamics of the shallow donors. For comparison the data of Lile, et al.[7] are presented with the results as calculated above in Fig. 12. The essential features of the data seem to be adequately represented by this model.

The 300°K current drift behavior of the accumulation MISFET was calculated using the above model for a series of different deep acceptor concentrations as shown in Fig. 13. As can be observed from this figure the maximum permissible acceptor concentration for current drift which does not exceed 5% of the initial current value is about 2×10^{15} cm^{-3}.

Conclusion

The crucial question which can only be answered by further experimental work concerns the amount of time required for the deep acceptor levels to come to equilibrium after the application of a gate pulse. If the process occurs in less than a nanosecond then the filling of deep levels by electrons is clearly not causing the drift in channel current that has been observed. On the other hand if the process takes several days (not very plausible) it is also not of much technological interest. Only if the capture cross sections are such as to make the effect observable over a time interval from about 10^{-8} to 10^{4} sec will the effect be important to circuit designers. In the present calculations the capture cross section has been treated as a curve fitting parameter - no independent measurements of capture cross sections for these deep levels are available. It is clearly important to obtain such data. The values of the impurity capture cross sections used in these calculations are considerably smaller than those quoted by Henry and Lang[25] for GaAs and GaSb. Until we have such data for InP, it will be difficult to determine if the values used for the present calculations are realistic or not.

The alert reader will have noted that early in the paper I made the point that the calculations of Okamura and Kobayashi give the correct temperature dependence of the current drift only if they neglect the principle of detailed balance in their formulation of the rate equation to describe the capture and

emission of electrons from traps in the oxide. Then at a later stage I have invoked essentially the same mathematical formalism to describe the capture of electrons by deep levels in the semiconductor through a multiphonon emission process. How do we know where the charge trapping is occurring? Is it in the insulator or in the semiconductor? Given the available data the possibility of drift due to traps in the oxide cannot be eliminated, however, it can be argued that at least some of the observed drift is due to traps in the semiconductor. At very low temperatures (77°K) we see no drift-on any time scale. If the semiconductor traps were charging too rapidly to be observed at 300°K, we should at least see some evidence of their existence as the sample is cooled. Instead we see nothing - no drift. The calculations presented in this paper have shown that for deep acceptor densities in the range of 10^{16} cm^{-3} (a lower limit for the current materials technology) the effects of deep level charging are easily observable. Therefore at least some of the charging effects that are seen from 77°K upward must be due to charging of states in the semiconductor.

In the present calculations only the effects of uniform impurity densities have been considered. If greater densities of deep levels are caused near the interface due to processing induced damage then even stronger effects would result than those predicted from estimates of the bulk iron density. Such results would also be observed if the processing were to induce the pile-up of iron near the surface.

Obviously a need exists for those people working on InP devices to begin to carefully evaluate the acceptor and donor densities in semi-insulating starting material before trying to draw conclusions on the efficacy of various surface preparation and insulator growth procedures in producing improved InP accumulation-type transistors. Such measurements are at the moment time

consuming and tedious and vendors of InP cannot be relied upon to provide such information. However, there seems to be no alternative if we are to make further progress in developing this device.

Acknowledgments

I wish to express my gratitude for financial support for this work from the Naval Research Laboratory under grant #N00014-82-K-2032. I also wish to thank H. H. Wieder for several useful suggestions during this effort.

References

1. L. G. Meiners, J. Vac. Sci. Technol. 15, 1402(1978).
2. G. Weimann, Thin Solid Films 56, 173(1979).
3. L. G. Meiners, J. Vac. Sci. Technol. 19, 373(1981).
4. D. L. Lile and D. A. Collins, Thin Solid Films 56, 225(1979).
5. K. P. Pande and D. Gubierrez, Appl. Phys. Lett. 46, 416(1985).
6. L. G. Meiners, D. L. Lile and D. A. Collins, Electron. Lett. 15,578(1979).
7. D. L. Lile, M. Taylor and L. Meiners, Japan. J. Appl. Phys. 22, 389(1982).
8. D. L. Lile and M. J. Taylor, J. Appl. Phys. 54, 260(1983).
9. S. M. Goodnick, T. Hwang and C. W. Wilmsen, Appl. Phys. Lett.
10. M. Okamura and T. Kobayashi, Japan. J. Appl. Phys. 19, 2143(1980).
11. E. Yamaguchi, M. Minakata and Y. Furukawa, apan. J. Appl. Phys. 23,L49(1984).
12. H. H. Wieder, IEEE Electron Device Lett. EDL-4, 108(1983).
13. F. P. Heiman and G. Warfield, Trans. Electron. Devices, ED-12, 167(1965).
14. J. F. Wager. K. Geib, C. W. Wilmsen and L. L. Kazmerski, J. Vac. Sci. Technol., B1, 778(1983).
15. H. Koelmans and H. C. DeGraaff, Solid-State Electron. 10, 497(1967).
16. W. Shockley and W. T. Read, Phys. Rev. 87, 835(1952).
17. J. S. Blakemore, Semiconductor Statistics, p. 118, Pergamon Press, New York, 1962.
18. E.W. Williams, W. Elder, M.G. Astles, M. Webb, J.B. Mullin, B. Straughan, and P.J. Tufton, J. Electrochem. Soc. 120, 1741(1973).

19. R. Schachter, D.J. Olego, J.A. Baumann, L.A. Bunz, P.M. Raccah, and W.E. Spicer, Apply. Phys. Lett. 47, 272.(1985).

20. R. Siewatz and M. Green, J. Appl. Phys. 29, 1034(1958).

21. S. D. Conte and C. deBoor, Elementary Numerical Analysis: An Algorithmic approach, p. 365, McGraw Hill, New York, 1972.

22. K. Huang and A. Rhys, Proc. R. Soc., London A204, 406(1951).

23. R. Kubo and Y. Toyozawa, Prog. Theor. Phys. 13, 160(1955).

24. G. Rickayzen, Proc. R. Soc., London A204, 480(1957).

25. C.V. Henry and D.V. Lang, Phys. Rev. B 15, 989(1977).

26. R. Kubo, Phys. Rev. 86, 929(1952).

Figure Captions

Figure 1. Cross sectional view of accumulation-type MISFET on InP.

Figure 2. Channel current as a function of time for an accumulation-type MISFET on InP, after Lile, et al.[7] Channel length 4 μm, channel width 400 μm, oxide thickness 100 nm, gate voltage 4 v, drain voltage 2 v.

Figure 3a. Energy band diagram for the native oxide on InP as proposed by Goodnick, et al.[9] with gate voltage equal to zero.

Figure 3b. Energy band diagram for the native oxides on InP with a positive gate voltage.

Figure 4. Energy band diagram for the tunneling model proposed by Okamura and Kobayashi[10]

Figure 5. Energy band diagram for an accumulated surface on semi-insulating InP.

Figure 6. Surface electric field vs. surface potential at $t = 0$ and $t = \infty$ for InP with $N_a = 5x10$ cm^{-3}, $N_d = 1x10^{16}$ cm^{-3} and $T = 300°K$. The dashed lines represent the boundary condition, $V_g = \psi_s + \epsilon_s E_s / C_{ox}$ = constant, for various values of the gate voltage, V_g. As time increases from $t = 0$ the solution for the system will move along a line of constant gate voltage from the curve representing the initial state to the curve representing the final state.

Figure 7. Surface electric field vs. surface potential at $t = 0$ and $t = \infty$ for InP with $N_a = 5x10^{[17}$ cm^{-3}, $N_d = 1x10^{16}$, and $T = 300°K$.

Figure 8. Plots of electric field and surface potential vs. distance from the semiconductor surface at $t = 0$ and $t = \infty$. N_d is $1x10^{15}$ cm^{-3}, N_a is $5x10^{16}$ cm^{-3}, and T is 300°K.

Figure 9. Dependence of initial and first values of the charge in the conducting channel of an accumulation-type MISFET on the deep acceptor doping. The dashed lines represent initial values and the solid lines represent final values. The dielectric thickness is 100 nm, the relative dielectric constant is 4, N_d is 10^{15} cm^{-3} and T is 300°K.

Figure 10. Time dependence of the channel current for an accumulation-type MISFET assuming a Shockley-Read type of rate equation. V_g is 4 v, the dielectric thickness is 100 nm, the relative dielectric constant is 4, σ_n(donor states) is 1.25×10^{-26} cm^2 and σ_p (acceptor states) is 1.25×10^{-26} cm^2.

Figure 11. Configuration coordinate diagram for a deep level trap. The energy (U) of the total system of the lattice plus one electron is plotted as a function of a generalized lattice coordinate (Q) and is plotted for the case when the electron is free (upper curve) and for the case when the electron is trapped (lower curve). E_0 represents the energy barrier for electron capture and E_I represents the energy for electron emission. The energy for optical emission from the minimum energy, Q', of the system when the electron is trapped to the conduction band is given by E_2.

Figure 12. Charge in the conducting channel of an accumulation-type MISFET as a function of time assuming that electron capture by the deep acceptor takes place via a multiphonon emission process. The crosses represent data taken by Lile, et al.[7] N_d is 1.1×10^{17} cm^{-3}, σ_n(donor) is 1.25×10^{-26} cm^2, σ_p (acceptor) is 1.25×10^{-30} cm^2, and $\mu_{fe} = 1230$ cm^2 v^{-1} s^{-1}.

Figure 13. Charge in the conducting channel of an accumulation-type MISFET as a function of time for deep acceptor concentrations between 10^{15} cm^{-3} and 10^{18} cm^{-3} assuming that the electron capture takes place via a multiphonon emission process. N_d is 10^{15} cm^{-3} and T is 300°K.

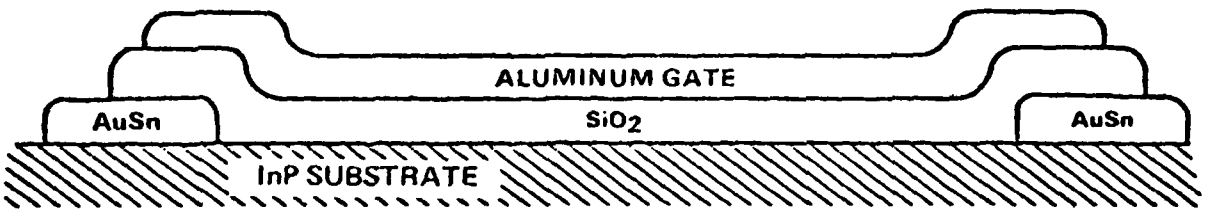

Fig 1

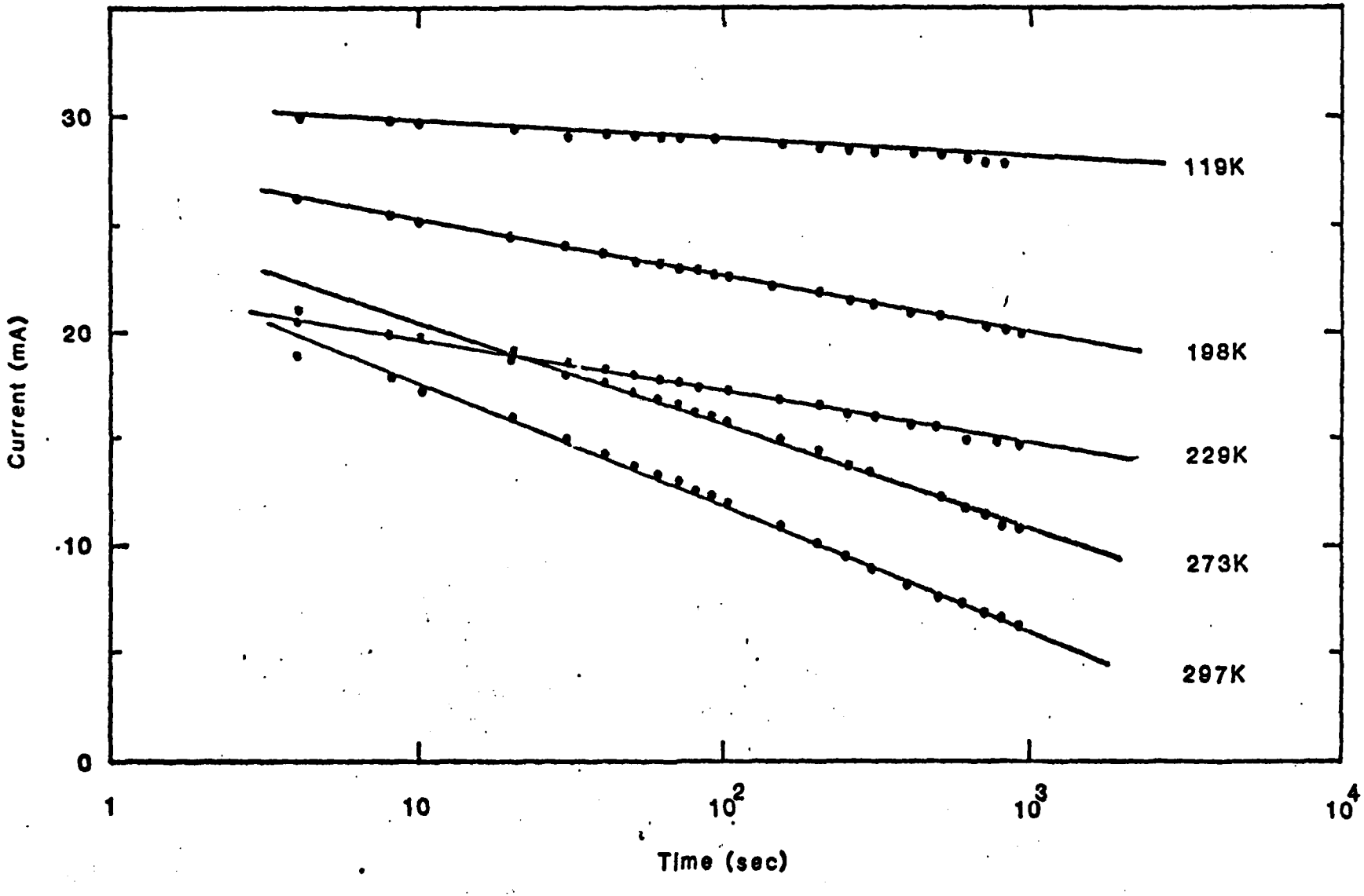
30
20
10
0
Current (mA)
1
10
10^2
10^3
10^4
Time (sec)
119K
198K
229K
273K
297K

Fig 2

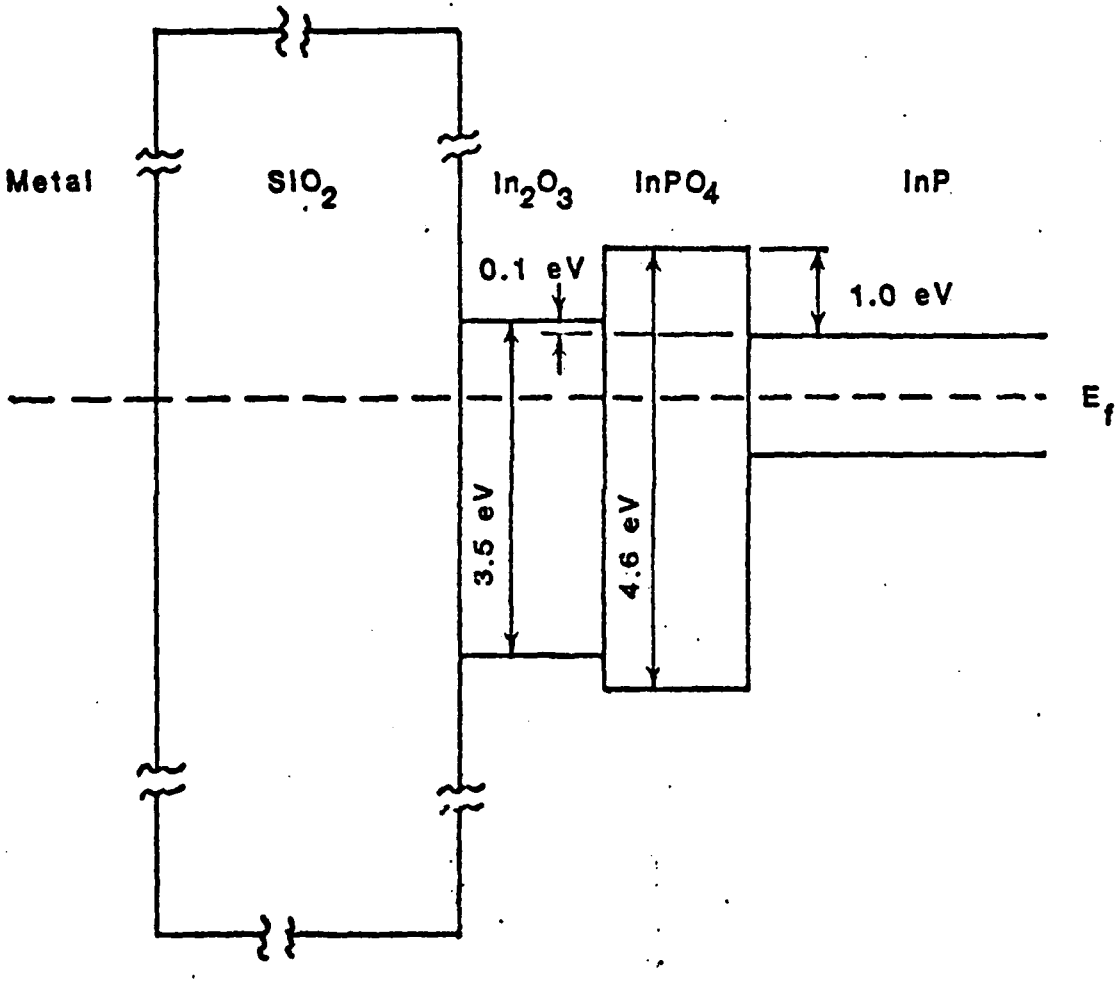

Fig 3c

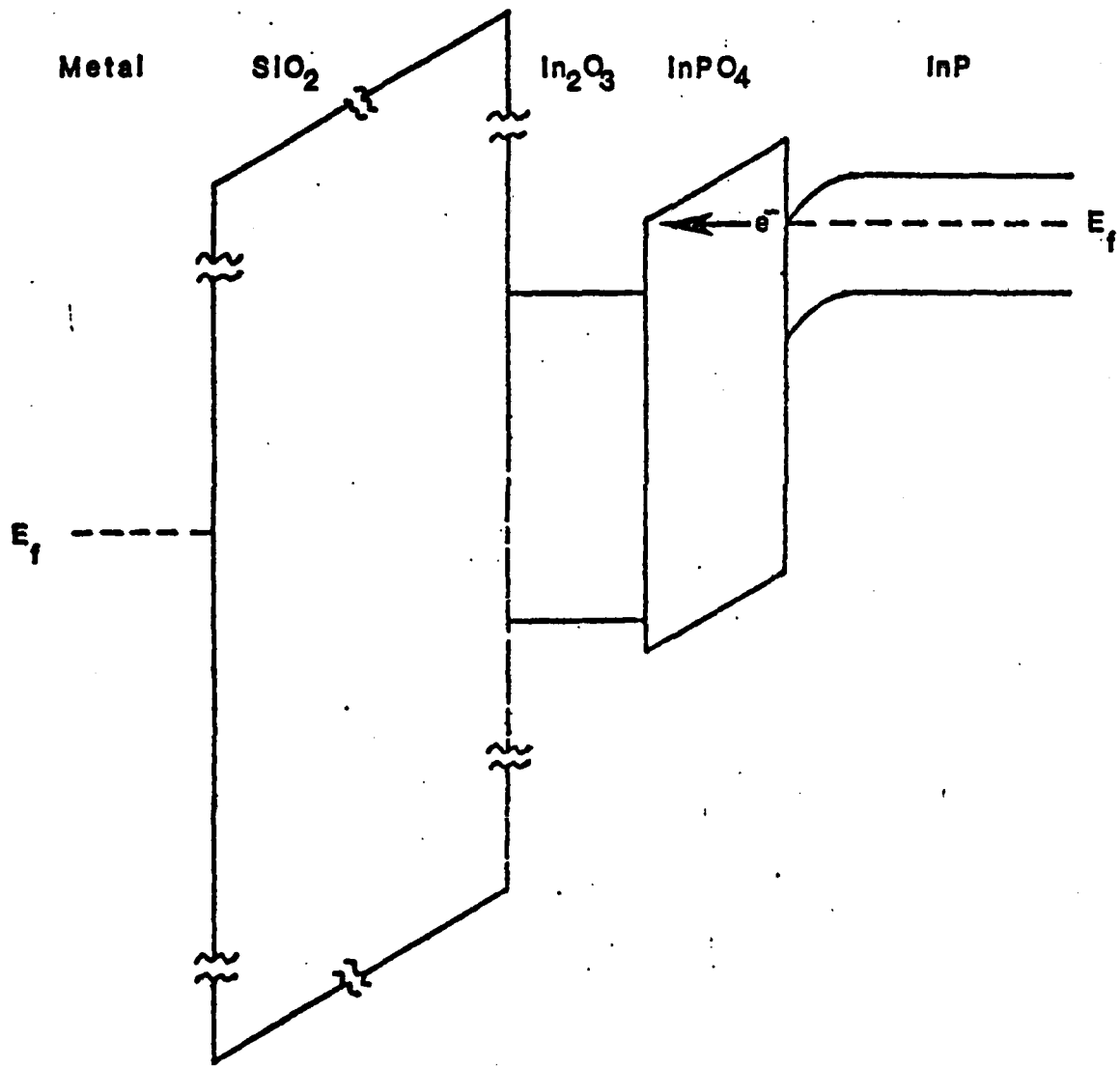

Fig 3b

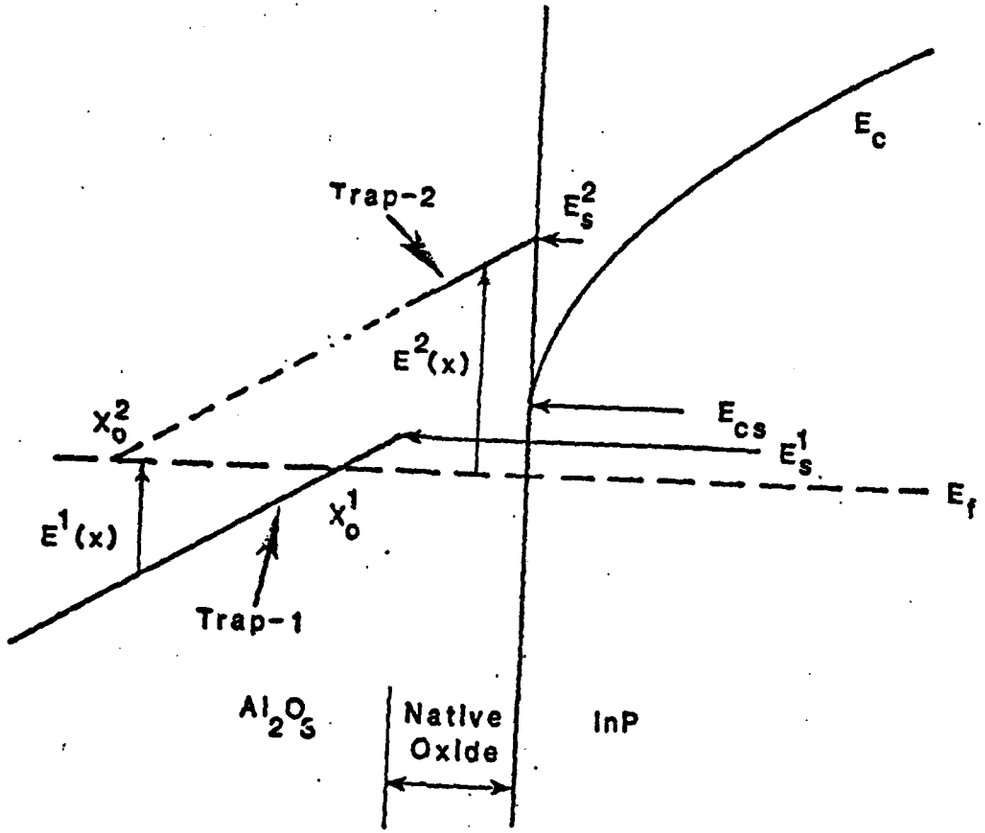
E_c
Trap-2
E_s^2
$E^2(x)$
X_o^2
E_{cs}
E_s^1
E_f
$E^1(x)$
X_o^1
Trap-1
Al_2O_3
Native Oxide
InP

Fig. 4

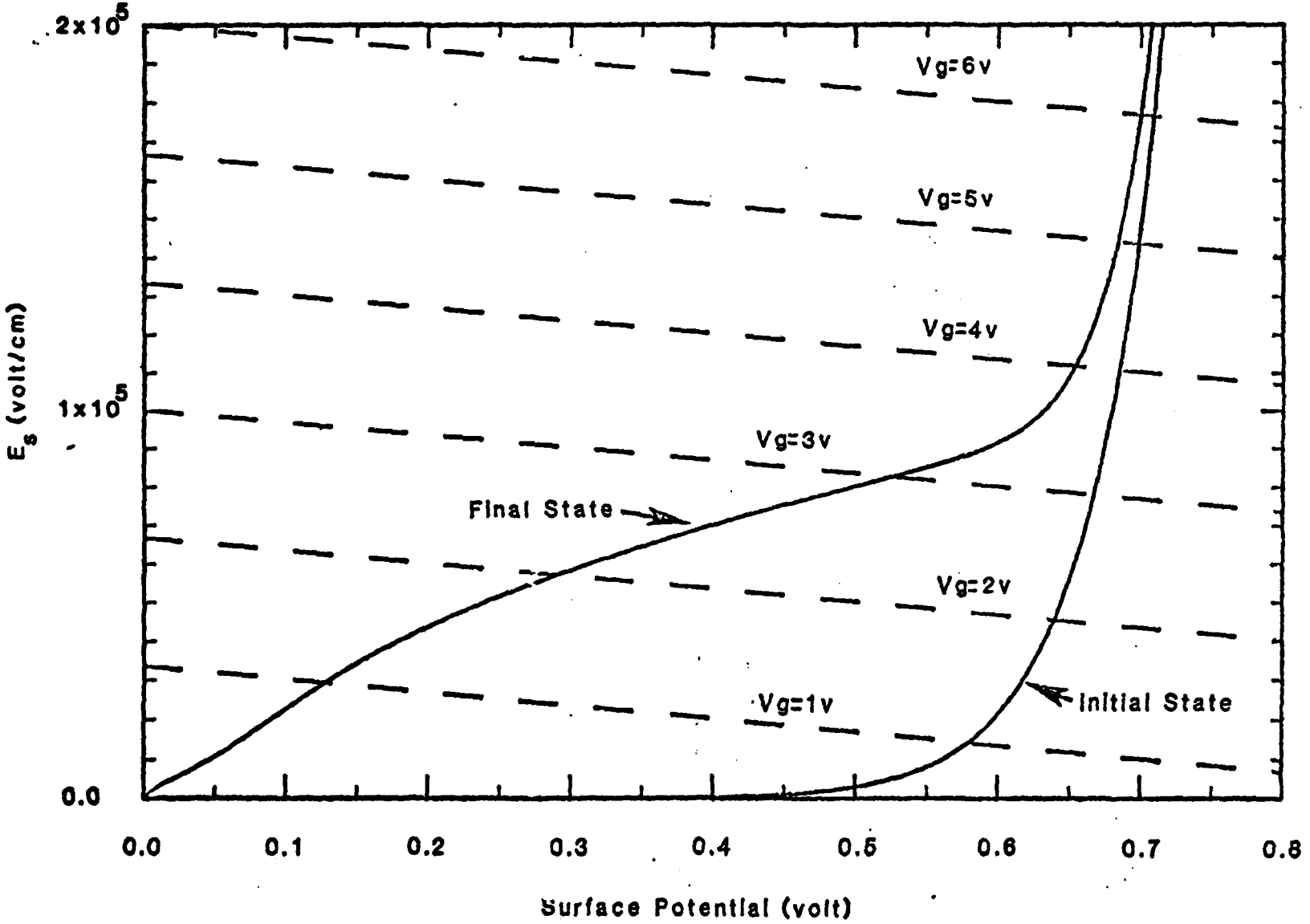
2x10^5
1x10^5
0.0
E_s (volt/cm)
Vg=6v
Vg=5v
Vg=4v
Vg=3v
Vg=2v
Vg=1v
Final State
Initial State
0.0
0.1
0.2
0.3
0.4
0.5
0.6
0.7
0.8
Surface Potential (volt)

Fig 6

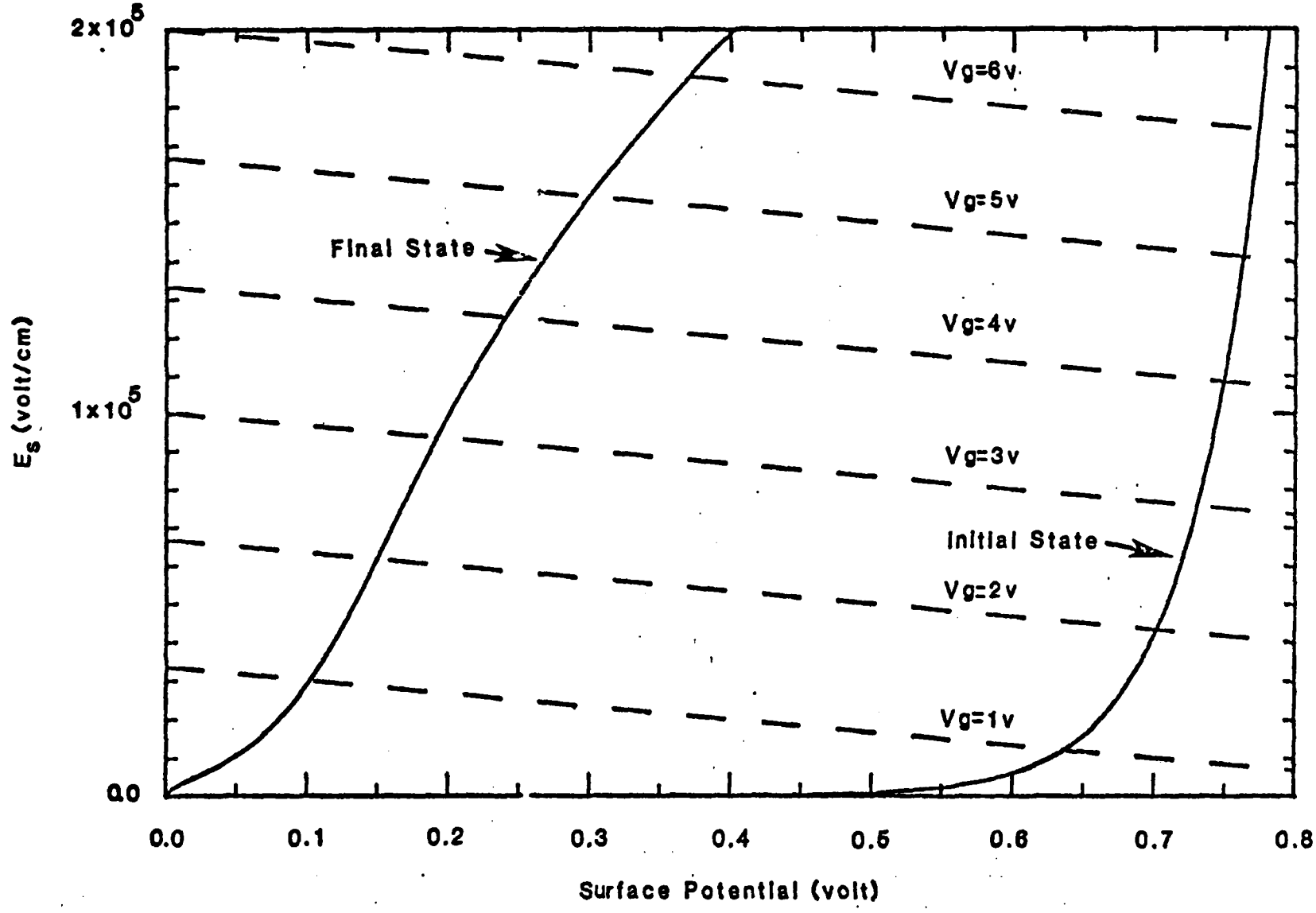
2x10^5
1x10^5
0.0
E_s (volt/cm)
Vg=6v
Vg=5v
Final State
Vg=4v
Vg=3v
Initial State
Vg=2v
Vg=1v
0.0
0.1
0.2
0.3
0.4
0.5
0.6
0.7
0.8
Surface Potential (volt)

Fig 2

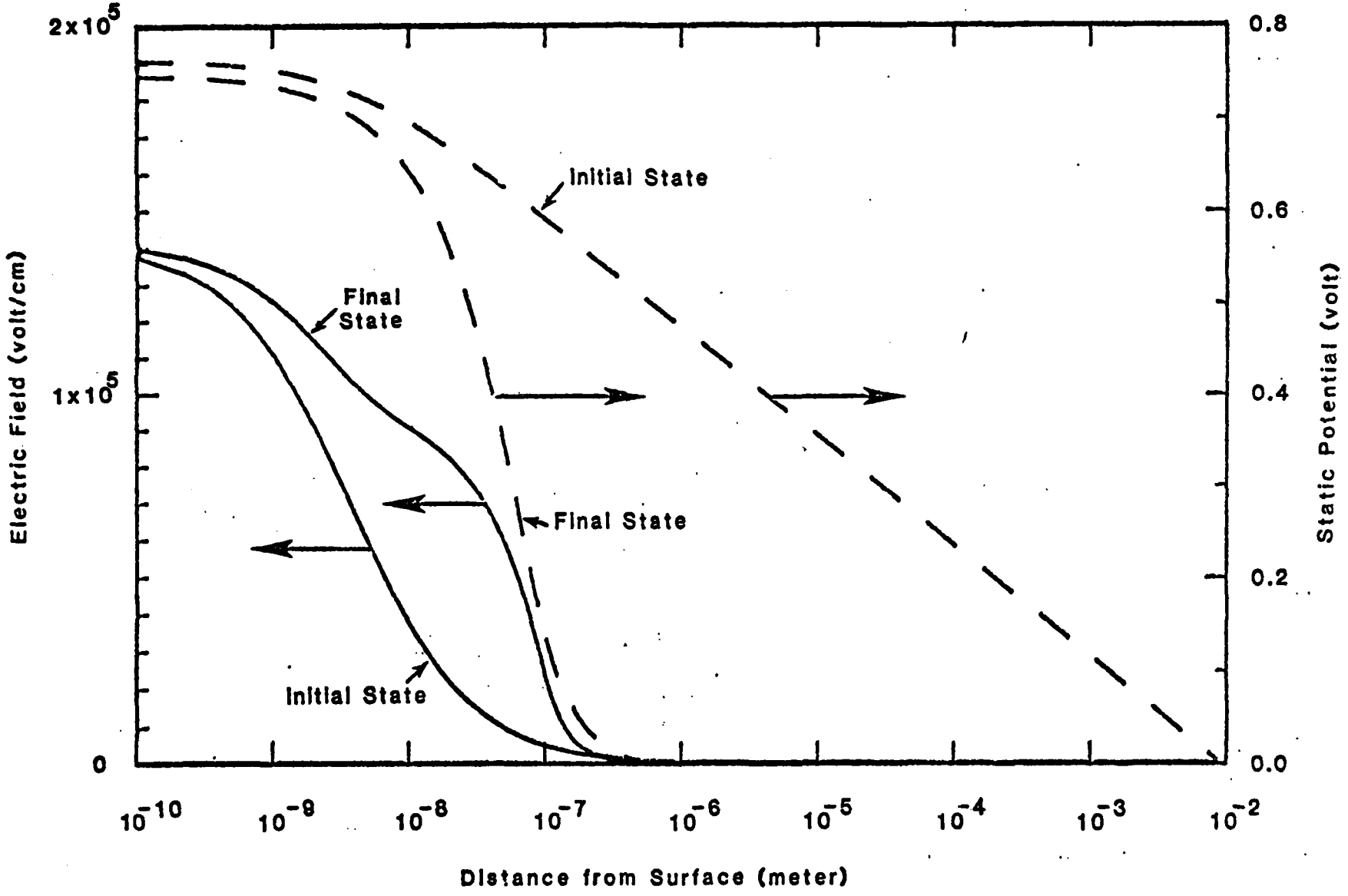
2x10^5
1x10^5
0
Electric Field (volt/cm)
0.8
0.6
0.4
0.2
0.0
Static Potential (volt)
Initial State
Final State
Final State
Initial State
10^-10
10^-9
10^-8
10^-7
10^-6
10^-5
10^-4
10^-3
10^-2
Distance from Surface (meter)

Fig 8

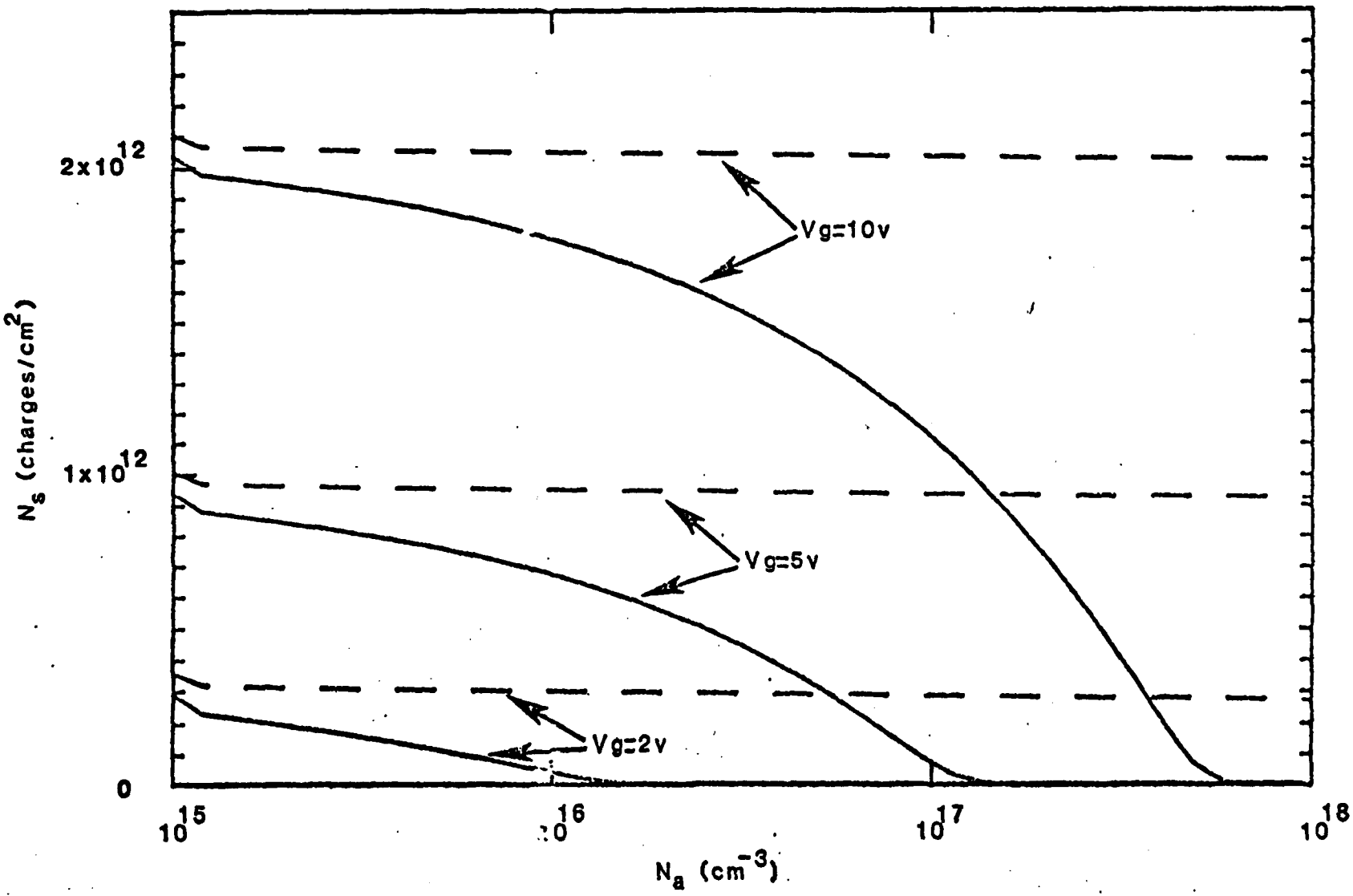
2x10^12
1x10^12
0
N_s (charges/cm^2)
Vg=10v
Vg=5v
Vg=2v
10^15
10^16
10^17
10^18
N_a (cm^-3)

Fig 9

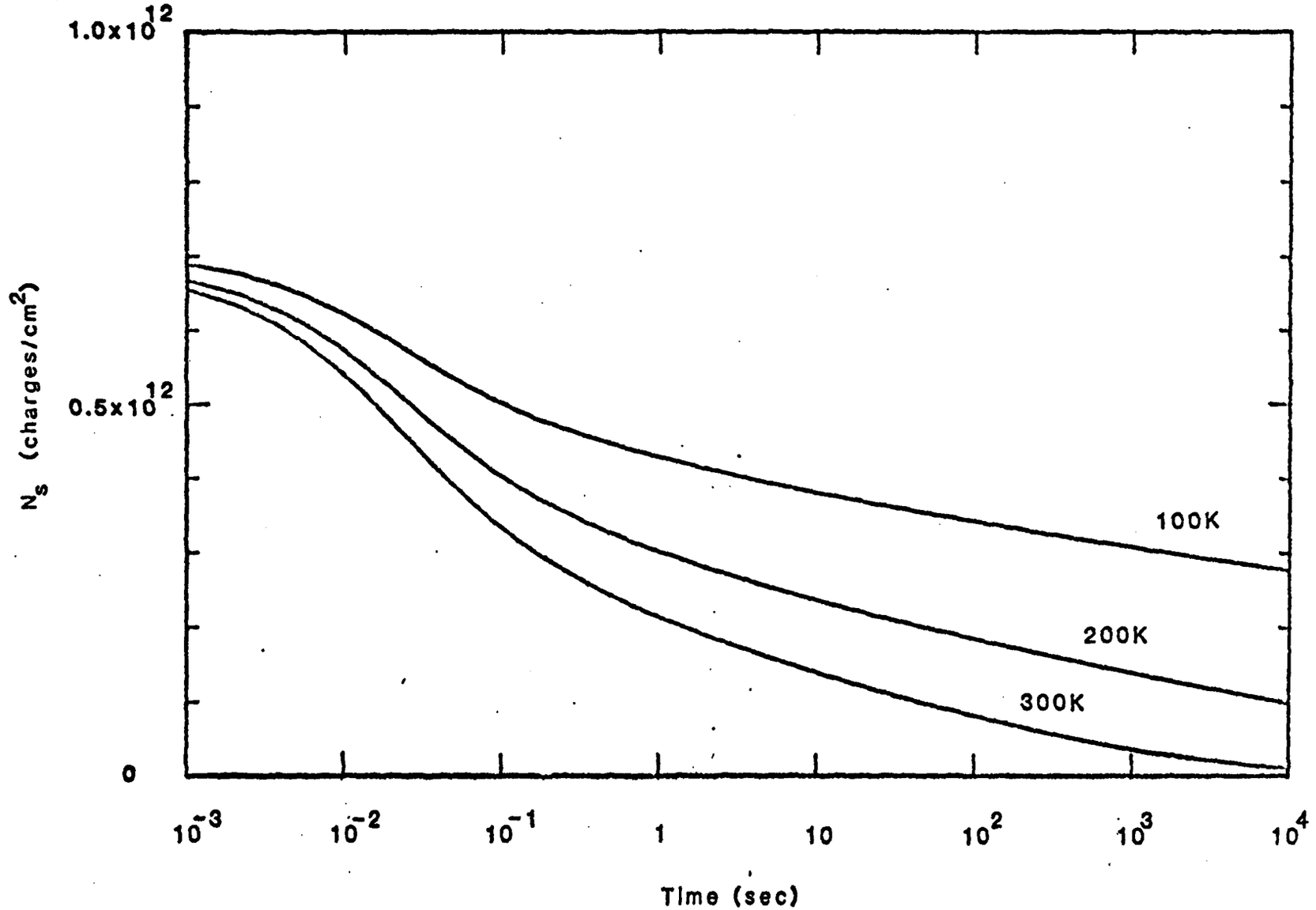
1.0x10^12
0.5x10^12
0
N_s (charges/cm^2)
100K
200K
300K
10^-3
10^-2
10^-1
1
10
10^2
10^3
10^4
Time (sec)

Fig 10

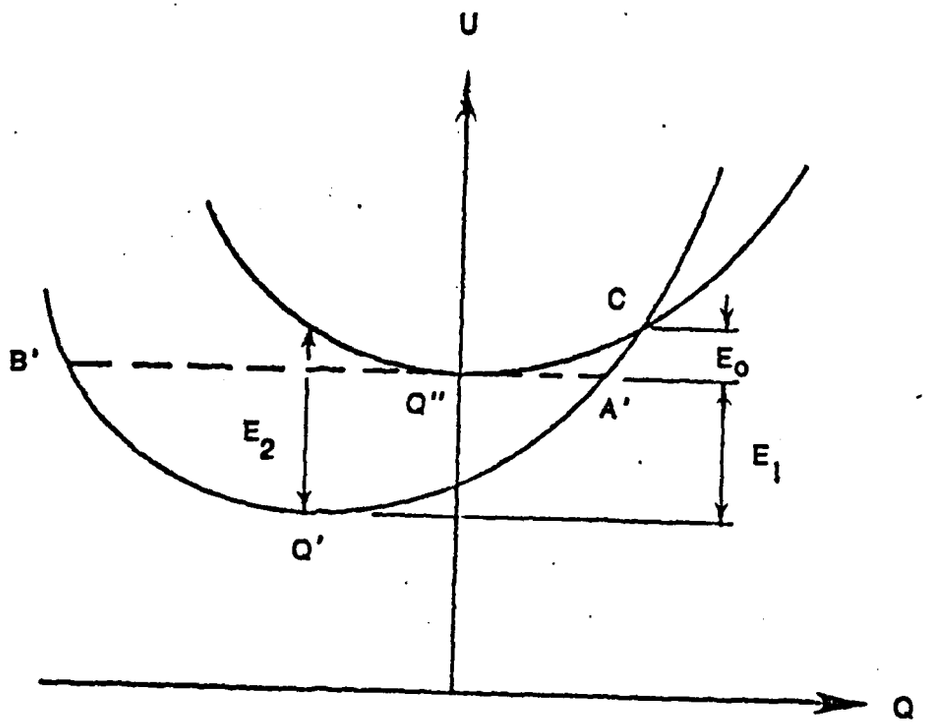

Fig 11

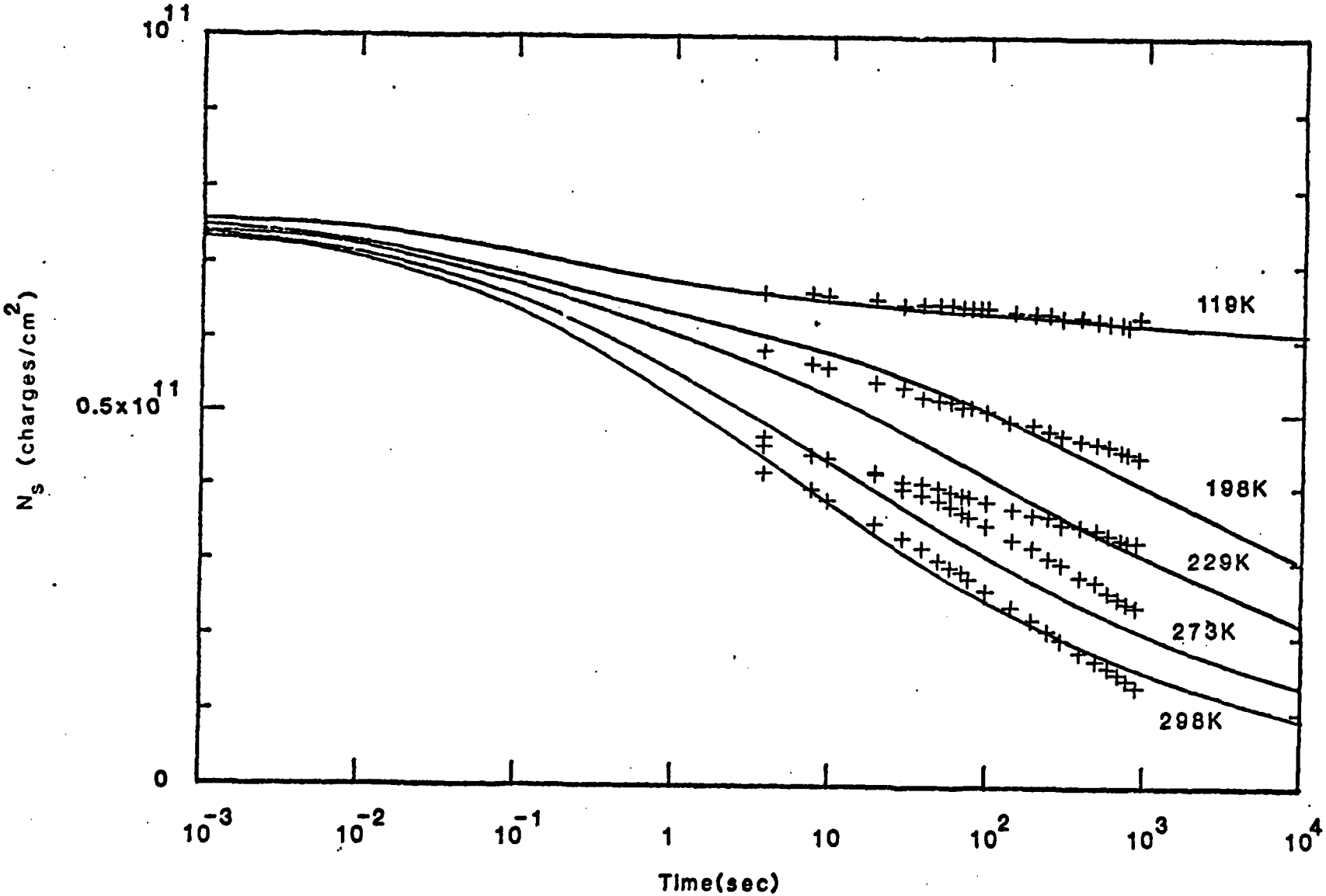
10^{11}
$0.5x10^{11}$
0
N_s (charges/cm^2)
119K
198K
229K
273K
298K
10^{-3}
10^{-2}
10^{-1}
1
10
10^2
10^3
10^4
Time(sec)

Fig 12

Space-Charge-Limited Currents and Trapping in Semi-Insulating InP

J. W. ROACH AND H. H. WIEDER

Abstract—The energy level and the density of the deep acceptor Fe^{3+} trap involved in space-charge-limited current (SCLC) flowing in semi-insulating (SI) InP was deduced from I–V measurements and a model employing either the low-field Hall mobility or the high-field saturated electron velocity v_s. The modified model based on v_s yields the Fe^{3+} energy level, $E_t = 0.6$ eV, and the trap density, $N_t = 3 \times 10^{15}$ cm^{-3}, consistent with data obtained by other means.

THE INTERACTION and parasitic coupling between adjacent field-effect transistors on their common semi-insulating (SI) GaAs substrates has led to detailed investigations of charge carrier transport in these substrates. Measured current versus voltage (I–V) data have been interpreted in terms of models which include [1]–[5] space-charge-limited current (SCLC) mediated by trapping, space-charge domain formation, impact ionization in high electric fields, and, more recently, self oscillation [6], [7] associated with field-dependent trapping. In SI GaAs the main electron trap EL-2 which is a deep donor level and compensates shallow residual acceptors has a significant effect on its I–V characteristics. In SI InP residual shallow donor levels are compensated by deliberately introduced Fe^{3+} deep acceptors. Although qualitative similarities are expected between SI GaAs and SI InP, the differences between the type and characteristics of their deep-level traps were expected to lead to observable differences in their charge carrier transport properties. In view of the applications of SI InP for electronic and electrooptic integrated circuit substrates investigations similar to those performed on SI GaAs were undertaken.

Au–Ge eutectic contacts, 350 μm × 130 μm, were vacuum deposited and annealed on the surface of liquid-encapsulated Czochralski-grown polished (100)-oriented Fe-doped SI InP which is slightly n-type with resistivity $\rho = 6 \times 10^7$ Ω·cm and electron mobility $\mu = 1500$ cm^2/V·s determined from low-field Hall measurements. The dc current–voltage characteristics were measured at room temperature under control of an HP 87XM computer using an HP 6034A programmable dc power source and a Keithley 619 programmable electrometer/multimeter to measure the current. Fig. 1 shows the I–V data of a representative specimen with 5-μm separation between the contacts. It is qualitatively similar to that of SI GaAs without the sharp inflection point of the current at the onset of the trap filled limit [8]. The onset of the trap filled limit is an order of magnitude higher than that obtained on SI GaAs with comparable contact spacing.

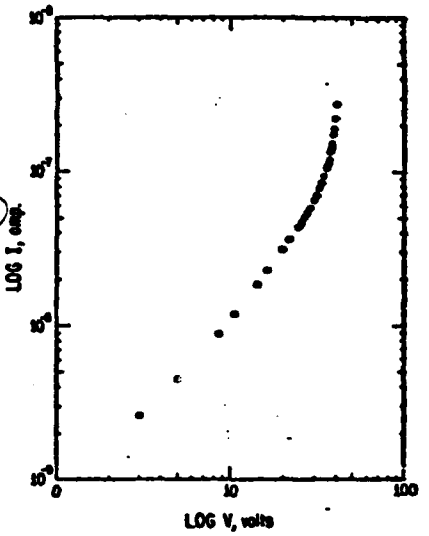

Fig. 1. Current–voltage curve for Fe-doped SI InP, with Au–Ge contacts separated by 5 μm, showing characteristic SCL form.

Interpretation of SCLC in SI GaAs has been based, as a rule, on the one-dimensional single carrier transport model of Lampert and Mark [8] which requires the assumption of a particular trap level and of its energy distribution. A straightforward method which provides the trap energy with no *a priori* assumption was described by Pfister [9] and further developed by Manfredotti *et al.* [10]. We have used this method to analyze the data shown in Fig. 1. Starting with Ohm's law and the one-dimensional Poisson's equation

$$J = e\mu nE$$
$$\epsilon(dE/dx) = \rho \tag{1}$$

where J is current density, e the electron charge, μ the free carrier mobility, n the concentration of free carriers, E the electric field, ϵ the dielectric permittivity of the material, and ρ the total charge density. Assuming a constant carrier mobility μ, a spatially homogeneous trap distribution, and a constant electrical length L between contacts, one obtains [9]

$$n_a = \frac{L}{e\mu}\left[\frac{d(V/J^2)}{d(1/J)}\right]^{-1} \tag{2}$$

where n_a is the free carrier density at the anode ($x = L$) and

Manuscript received March 29, 1985; revised May 3, 1985. This work was supported by the Naval Research Laboratory.

The authors are with the Department of Electrical Engineering and Computer Sciences, C-014, University of California, San Diego, La Jolla, CA 92093.

0741-3106/85/0700-0356$1.00

V the applied potential. The quasi-Fermi level E_F at the anode is then determined from

$$E_F = kT \ln \frac{N_c}{n_a} \tag{3}$$

with E_F considered positive going downward from the conduction band, and N_c the conduction-band density of states, k Boltzman's constant, and T the absolute temperature. The total charge density at the anode ρ_a may be found from

$$\rho_a = \frac{\epsilon}{L^2} \frac{d}{d(1/J)} \left[\frac{d(V/J^2)}{d(1/J)} \right]. \tag{4}$$

If trapped charge dominates then, with $n_t \simeq (1/e)\rho_a$

$$\frac{1}{e} \frac{d\rho_a}{dE_F} \simeq \frac{dn_t}{dE_F} \tag{5}$$

where n_t is the density of trapped carriers at the anode. (Trapped charge dominance corresponds to $e^{-1}\rho_a \simeq n_t \gg n_a$). If a discrete electron trap of energy E_t and total concentration N_t is present then

$$n_t = \frac{N_t}{1 + \frac{1}{g} \exp\left(\frac{E_F - E_t}{kT}\right)} \tag{6}$$

where g is the spin degeneracy factor. dn_t/dE_F (not n_t!) will have its maximum at

$$E_{F\max} = E_t + kT \ln g = E_t \tag{7}$$

with a value of

$$\left.\frac{dn_t}{dE_F}\right]_{E_{F\max}} = \frac{N_t}{4kT}. \tag{8}$$

(Assuming that $g = 2$ and that $kT \ln g$ is roughly 0.02 eV at room temperature then it is usually sufficient to state that $E_t \simeq E_{F\max}$). Thus, from the position of the maximum $E_{F\max}$, and from the value of the maximum itself, E_t and N_t may be obtained, respectively. A simple check that E_T is discrete made by means of (5) and (6) is

$$n_t]_{E_{F\max}} = N_t/2. \tag{9}$$

Hence, if N_t obtained from (8) agrees with that obtained from (9), then the level is likely to be discrete. An additional check is that the full width at half maximum (FWHM) of dn_t/dE_F for (5) is

$$\text{FWHM of } dn_t/dE_F = 3.5\ kT \tag{10}$$

which is approximately 0.09 eV at room temperature.

One drawback to the use of (2), (4), and (5) is that multiple derivatives of the experimental I–V curve must be determined; the errors and fluctuations in the data are multiplied with each derivative.

A simplified version of this method [10] assumes that the electric field at the anode is essentially twice the "ohmic" electric field V/L. In that case, (2) and (4) simplify to

$$n_a = \frac{JL}{2e\mu V} \tag{11}$$

and

$$\rho_a = \frac{2\epsilon V}{L^2} \tag{12}$$

respectively. Using (3), (5), (11), and (12) dn_t/dE_F be expressed directly in terms of the current density and voltage as

$$\frac{dn_t}{dE_F} = \frac{2\epsilon}{ekTL^2} \left(\frac{JV}{J - V \cdot \frac{dJ}{dV}} \right). \tag{13}$$

This greatly simplifies calculation, in that only the first derivative of the I–V curve need be obtained. Equations (3) and (5)–(10) are unchanged.

This simplified version was applied to the I–V data, shown in Fig. 1, with $\mu = 1500\ \text{cm}^2/V\cdot\text{s}$, $\epsilon = 1.1 \times 10^{-12}$ F/cm (corresponding to a dielectric constant of 12.4), $N_c = 5.4 \times 10^{17}/\text{cm}^3$, and $L = 5\ \mu\text{m}$. J was replaced by I/A where A is the contact area, 350 μm × 130 μm. (dI/dV) was calculated numerically, and some smoothing of the I–V data was required to attenuate fluctuations. Fig. 2 shows the resultant dn_t/dE_F versus E_F plot. From (7), a trap energy level of $E_t = 0.66$ eV is obtained, and from (8) and the peak value of dn_t/dE_F ($6.8 \times 10^{16}/\text{cm}^3\cdot\text{eV}$), its density N_t is $7 \times 10^{15}/\text{cm}^3$. It is in disagreement with that determined from n_t versus E_F in the same figure, and (8), $N_t = 2.4 \times 10^{15}/\text{cm}^3$. Furthermore, the FWHM of dn_t/dE_F is 0.03 eV, less than the 0.09 eV expected for a discrete level. It is, however, in good agreement with the thermal activation energy determined by Mizuno *et al.* [12].

The electron velocity of InP reaches a peak value for an electric field, $E = 11$ kV/cm, which for a 5-μm contact separation is -5 V. The maximum voltage of Fig. 1, 40 V, is well beyond this saturation limit and a constant electron velocity v_s, rather than a constant mobility may be assumed applicable to SI InP with

$$J = env_s. \tag{14}$$

With $\nabla \cdot J = dJ/dx = 0$, and v_s constant, n does not depend on x, and

$$\rho = 2\epsilon V/L^2 \tag{15}$$

where the potential $V = -\int_0^L E dx$. Equations (3) and (5) are still applicable, and with (14) solved for n, there follows from (15):

$$\frac{1}{e} \frac{d\rho}{dE_F} = \frac{dn_t}{dE_F} = \frac{2\epsilon l}{ekTL^2} \cdot \frac{dV}{dI}. \tag{16}$$

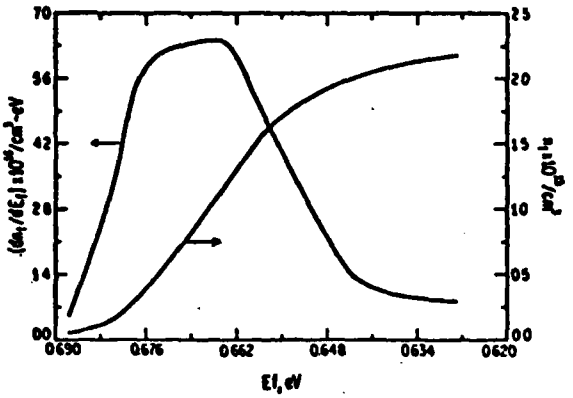

Fig. 2. Occupied trap concentration n_t, and change in occupied trap concentration with Fermi level dn_t/dE_F versus Fermi level E_F, for the data from Fig. 1 assuming constant mobility.

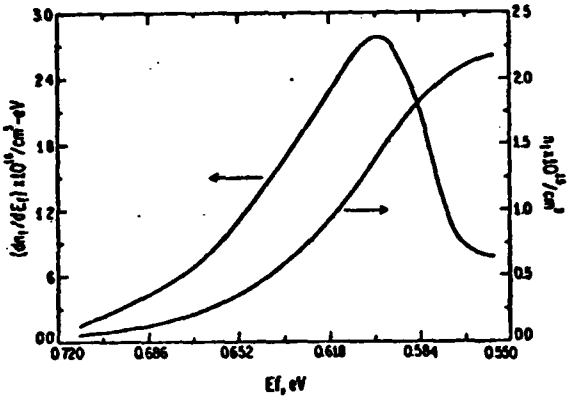

Fig. 3. Occupied trap concentration n_t, and change in trap concentration with Fermi level dn_t/dE_F versus Fermi level E_F, for the data from Fig. 1 assuming constant carrier velocity.

This modified version was applied to the I–V data in Fig. 1 and the dn_t/dE_F versus E_F plot obtained therefrom is shown in Fig. 3. The saturated electron velocity v_s, used was 1.5×10^7 cm/s, consistent with theoretically calculated and experimentally verified values of n-types InP [11].

From Fig. 3 and the appropriate equations (7)–(10), $E_t = 0.60$ eV (below the conduction band edge) and $N_t = 3 \times 10^{15}/\text{cm}^3$.

These results may be compared to the activation energy of Fe^{3+} in SI InP of 0.64 eV determined by Fung *et al.* [12] using photoconductive measurements and with that of Zeisse *et al.* [13] of 0.53 eV using galvanomagnetic measurements. The iron concentration in SI InP, determined from secondary ion mass spectroscopic measurements [13], is 3×10^{15}–$10^{16}/\text{cm}^3$ (within a factor of two), in fair agreement with our data. The FWHM of $dn_t/dE_F = 0.07$ eV is much closer to the expected 0.09 eV. We tend to favor, therefore, the constant electron velocity data of Fig. 3 which yields $E_t = 0.6$ eV.

In conclusion, a direct method intended for the evaluation of the energy and density of traps involved in SCLC has been applied, in simplified form, to Fe-doped SI InP, assuming a constant electron mobility and a modified version for the possibly more realistic assumption of a saturated (constant) electron velocity. The results favor a single, discrete trap level located -0.6 eV below the band edge and a trap density of $\sim 3 \times 10^{15}/\text{cm}^3$ associated with the ionized Fe^{3+} deep level in InP.

REFERENCES

[1] C. P. Lee, S. J. Lee, and B. M. Welch, "Carrier injection and backgating effect in GaAs MESFET's," *IEEE Electron Device Lett.*, vol. EDL-3, pp. 97–98, 1982.

[2] M. F. Chang, C. P. Lee, L. D. Hou, R. P. Vahrenkamp, and C. G. Kirkpatrick, "Mechanism of surface condition in semi-insulating GaAs," *Appl. Phys. Lett.*, vol. 44, pp. 869–871, 1984.

[3] C. P. Lee, "Influence of substrates on the electrical properties of GaAs FET devices and integrated circuits," in *Semi-Insulating III–V Materials: Evian 1982*, S. Makram-Ebeid and B. Tuck, Eds. Cheshire, England: Shiva, 1982.

[4] C. Le Mouelic, S. Mottet, J-M. Dumas, and D. Lecrosnier, "Influence des défauts de surface sur le comportement des MESFET GaAs," *Rev. Phys. Appl.*, vol. 19, pp. 149–154, 1984.

[5] S. Makram-Ebeid and P. Minondo, "Effets parasites dans les transistors à effet de champ en GaAs: rôle de la surface et du substrat semi-isolant," *Acta Electronica*, vol. 25, pp. 241–260, 1983.

[6] M. Kaminska, J. M. Parsey, J. Lagouski, and H. C. Gatos, "Current oscillations in semi-insulating GaAs associated with field-enhanced capture of electrons by the major deep donor EL2," *Appl. Phys. Lett.*, vol. 41, pp. 989–991, 1982.

[7] G. N. Maracas, D. A. Johnson, and H. Goronkin, "Experimental evaluation of low-frequency oscillations in undoped GaAs to probe deep level parameters," *Appl. Phys. Lett.*, vol. 46, pp. 305–307, 1985.

[8] M. A. Lampert and P. Mark, *Current Injection in Solids*. New York: Academic, 1970, ch. 2, 4.

[9] J. C. Pfister, "Note on the interpretation of space charge limited currents with traps," *Phys. Stat. Sol.(a)*, vol. 24, pp K15–K17, 1974.

[10] C. Manfredotti, C. De Blasi S. Galassini, G. Micocci, L. Ruggiero, and A. Tepore, "Analysis of SCLC curves by a new direct method," *Phys. Stat. Sol.(a)*, vol. 36, pp. 569–577, 1976.

[11] K. Brennan and K. Hess, "High field transport in GaAs, InP and InAs," *Solid-State Electron.*, vol. 27, pp. 347–357, 1984.

[12] O. Mizuno and H. Watanabe, "Semi-insulating properties of Fe-doped InP," *Electron. Lett.*, vol. 11, pp. 118–119, 1975.

[13] S. Fung, R. J. Nicholas and R. J. Stradling, "A study of the deep acceptor levels of iron in InP," *J. Phys. C.: Solid State*, vol. 12, pp. 5145–5155, 1979.

[14] C. R. Zeisse, G. A. Antypas, and C. Hopkins, "Electron and iron concentration in semi-insulating indium phosphide," *J. Cryst. Growth*, vol. 64, pp. 217–221, 1983.

END

FILMED

11-85

DTIC